

Recent advances in two-photon imaging: technology developments and biomedical applications

Yu Chen^{1*}, Hengchang Guo^{1,2**}, Wei Gong^{1,3}, Luye Qin², Hossein Aleyasin², Rajiv R Ratan²,
Sunghee Cho², Jianxin Chen³, and Shusen Xie^{3***}

¹Fischell Department of Bioengineering, University of Maryland, College Park, MD 20742, USA

²Burke Medical Research Institute, Weill Medical College of Cornell University, White Plains, NY 10605, USA

³Institute of Laser and Optoelectronics Technology, Fujian Normal University, Fuzhou 350007, China

*Corresponding author: yuchen@umd.edu; ** corresponding author: hcguo@umd.edu;

*** corresponding author: sxxie@fjnu.edu.cn

Received October 30, 2012; accepted December 7, 2012; posted online January 6, 2013

In the past two decades, two-photon microscopy (TPM) transforms biomedical research, allowing non-destructive high-resolution fluorescent molecular imaging and label-free imaging *in vivo* and in real time. Here we review the recent advances of TPM technology including novel laser sources, new image acquisition paradigms, and microendoscopic imaging systems. Then, we survey the capabilities of TPM imaging of biological relevant molecules such as nicotinamide adenine dinucleotide (NADH), flavin adenine dinucleotide (FAD), and reactive oxygen species (ROS). Biomedical applications of TPM in neuroscience and cancer detection are demonstrated.

OCIS codes: 170.3880, 170.0170, 180.4315, 180.0180, 170.2150, 170.0170, 190.4180, 190.0190, 170.6510, 170.0170.

doi: 10.3788/COL201311.011703.

1. Introduction

Since the work of Denk *et al.* over 20 years ago^[1], two-photon microscopy (TPM) has become a key tool for biomedical research to observe cellular properties and functions. TPM is a form of light microscopy that uses localized nonlinear optical effects induced by two-photon excitation. The near-infrared (NIR) laser wavelengths used for TPM reduce tissue and water absorption. Together with the reduced scattering of the excitation light, TPM has led to penetration depths of over 1 mm into biological tissues^[2,3]. In addition, TPM reduces photo-bleaching, photo-damage and toxicity by spatially confining fluorescence excitation. With these advantages, studies have shown exponential growth in biomedical applications^[1,4–6]. TPM has provided unprecedented anatomical, cellular, molecular and functional information *in vivo*. Neuroscientists have used TPM for molecular imaging of calcium, nicotinamide adenine dinucleotide (NADH), flavin adenine dinucleotide (FAD), reactive oxygen species (ROS), oxygen, and fluorescent proteins in cells, tissues, and living animals to study neuronal plasticity, neuron dynamics, and monitor neurodegenerative diseases models^[7–15]. TPM has also enabled studies of tumor morphology, angiogenesis, and metastasis for cancer detection and therapy^[16–20]. Immunologists use TPM for investigating immune cell dynamics, lymphocyte trafficking and embryologists use TPM for visualizing the development of animal embryos^[21–25].

Two-photon fluorescence (TPF) imaging is usually the primary form of TPM. Other nonlinear optical effects have also been used for two-photon label-free biomedical imaging such as second harmonic generation (SHG), sum-frequency generation (SFG), and coherent Anti-Stokes Raman scattering (CARS)^[26,27].

In this review, we will introduce recent technical ad-

vances of laser sources, scanning schemes, and microendoscopes. In addition, representative biomedical applications such as preclinical mice stroke models diagnosis and early cancer detection are demonstrated.

2. Contrast mechanisms for TPM

2.1 TPF imaging

In the two-photon process, a molecule simultaneously absorbs two photons whose individual energy is only half of the energy state needed to excite that molecule, and then releases the energy to an emission fluorescence photon, a phosphorescence photon, or a SHG photon^[1,4,28]. TPF imaging can be achieved from two-photon excitation of fluorescent dyes, fluorescent proteins, and nanoparticles.

Fluorescent protein is a promising class of fluorophores which are easy to label target genes with strong fluorescence emission. The available fluorescent proteins have covered the emission wavelength from blue to NIR colors such as cyan fluorescent protein (CFP), green fluorescence proteins (GFP), yellow fluorescence proteins (YFP), dsRed, mCherry, tdTomato, eqFP670, etc.^[5,15,29–31]. GFP enabled scientists to detect chemical species such as metals ions and small molecules; even to visualize processes such as the development of neurons and the migration of cancer cells^[15,32,33].

Nanoparticles, such as quantum dots (QDs), gold nanoparticles, carbon dots, etc., are promising fluorescent labels for TPM^[34–37]. They have broad excitation spectra, narrow emission spectra, and excellent photostability^[34,37]. QDs are reported to have TPE cross-sections up to 47 000 Goeppert-Mayer units (GM), which is 2–3 orders of magnitude larger than those of conventional fluorescent probes^[34]. A major challenge

in the use of these nanoparticles is their large size and molecular specific targeting within the specimen^[34]. Furthermore, some fluorescent dyes and nanoparticles will induce toxicity in biological systems^[38–40].

In addition to exogenous fluorophores, TPM can image endogenous fluorescence molecules such as the reduced NADH, FAD, and keratin^[41–45]. TPF imaging of these molecules allows label-free imaging of unstained intact tissues, and therefore has great potential for future clinical translation to clinical studies.

2.2 Non-fluorescence imaging

Except for TPF imaging, nonlinear optical effects such as SHG, SFG, and CARS have been used for label-free imaging of biological tissues. SHG microscopy is used for biological specimens that consist of highly ordered but directionally asymmetric molecular assemblies, such as collagen or striated muscle fibers. These structures tend to produce strong SHG signals as a result of the dependence of frequency doubling on a broken spatial inversion symmetry within the sample material structure^[46]. Because SHG does not require absorption, it is often well-generated over a broader range of illumination wavelengths than those for fluorescence excitation. CARS microscopy creates images by using intrinsic signatures of molecular vibrations within the sample for contrast generation. A molecular vibration of interest is probed using nonlinear interactions in the sample between three photons from two laser beams, known as the pump beam and the Stokes beam, whose frequency difference is tuned to match the vibrational resonance. CARS imaging appears well-suited for examination of myelin sheaths and other lipid-rich tissues^[47,48].

3. Advanced two-photon microscope

The main differences between confocal microscopy and TPM are the excitation light source and the fluorescence detection unit. TPM, including all commercial versions, is typically implemented in a simple laser scanning microscope equipped with an ultrafast pulse laser, which is focused to a tight spot in the specimen plane and scanned in a raster pattern over the sample. Fluorescence photons or nonlinear optical signals (e.g. SHG) are generated selectively in the tiny focal volume $\sim 10^{-12}$ cm³ and detected by photodetectors such as photomultiplier tubes (PMTs) or avalanche photodiodes (APDs). The signals are recorded and mapped to individual pixels of an image. To discuss recent advances of the TPM system, we will focus on key technology developments in lasers, scanners, and microendoscopes.

3.1 Laser system

TPM depends on a high peak-power ultrafast laser system to efficiently induce nonlinear optical effects inside biospecimens. Most current sources are mode-locked solid-state lasers. A Ti:sapphire laser is generally used as an ultrafast pulse source with an average power over 1 Watt peak wavelength ~ 800 nm and a wide wavelength-tuning range of 690–1050 nm^[5,49].

The increasing translational potential of TPM motivates new trends of technology development including longer wavelength for deep tissue penetration^[2,3,50] and compact size for portable applications^[51–53]. There have been previous studies utilizing longer wavelength excitation, particularly using Cr:Forsterite lasers around 1.23 μm ^[54], Ti:Sapphire pumped optical parametric oscillator (OPO) sources around 1.06–1.45 μm ^[2,3,50] and optical parametric amplifier (OPA) source around 1240 nm^[55,56], 1.55- μm fiber lasers^[57,58], and supercontinuum light sources^[59]. Figure 1 shows deep depth *in vivo* TPM of a mouse brain cortex stained with Alexa680-Dextran using long wavelength laser pulses of 1280 nm^[2,3].

Another trend towards practical TPM system is the development of compact and turn-key light sources. The emerging compact laser systems are based on semiconductor laser-diode (LD) systems^[15,27,51–53,59,60], optical fiber laser systems^[57,58,61], and even chip-size devices^[62].

LD has been used as a reliable, low-cost, high-performance light source in scientific research, optical communication, and information technologies. For the promising applications of nonlinear optical imaging, Guo *et al.* developed high peak-power semiconductor laser

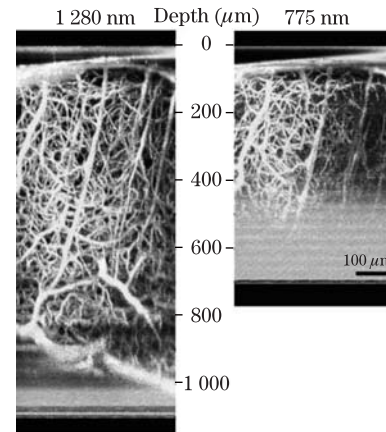


Fig. 1. TPM of mouse brain blood vessels at approximately twice the depth with 1280-nm excitation as with 775-nm excitation^[2]. Blood plasma is labeled by FITC-dextran and Alexa680-dextran.

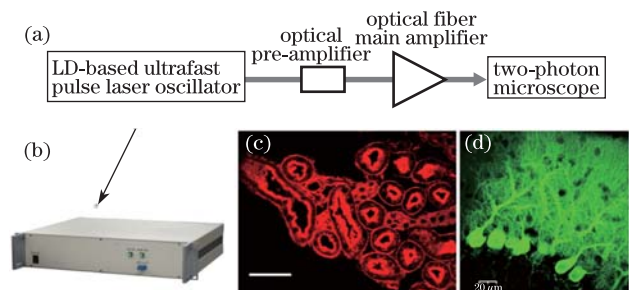


Fig. 2. (a) Schematic for high peak power ultrafast optical pulse source for TPM. (b) Photo of 500-MHz repetition rate, 2.7-ps pulse width, and 1- μm semiconductor laser oscillator^[15]. (c) TPM of convoluted tubules in mouse kidney tissues stained with Alexa Fluor 488 using all-semiconductor light source^[53]. (d) TPM of brain Purkinje cells express GFP using 1030-nm semiconductor light source^[15]. The scale bars are 50 μm in (c) and 20 μm in (d).

systems^[15,27,51–53]. In these systems, LDs serve as easily-operated devices for generating stable picosecond optical pulses. Subsequent use of low-noise optical pre-amplifier and low-nonlinear-effect optical main amplifiers raises the optical pulse peak power to more than a kilowatt, making it suitable for TPM. The experimental configuration for kilowatt peak power optical pulse generation and TPM is shown in Fig. 2. Ultrafast optical pulses with less than 5-ps duration are generated by again-switching or mode-locked LD. For nonlinear optical microscopy, low noise and low nonlinear effect optical fiber amplifiers were then developed for optical pulse generation with peak power up to the kilowatt level. Kilowatt peak-power picosecond laser pulses at 775, 800, and 1030 nm have been generated for TPF imaging of mouse kidney tissues and mouse brain neurons expressing GFP (Figs. 2(c) and (d))^[15,51,53].

3.2 Scanners

Conventional TPM employs a pair of galvanometric scanning mirrors for 2D raster scanning, and therefore is limited to line scans around 1–2 kHz, which could be slow for applications requiring high temporal resolution. Hence, random-access scanning using a device containing acousto-optic deflectors (AODs) has been developed^[63,64]. By tuning the input electric frequency applied on the acoustic crystal, AOD can change the laser beam deflection angle. Alternatively, parallel scanning with multiple beams can be implemented^[65–67]. More recently, scanless technique using temporal focusing has been developed^[68]. Instead of allowing laser pulses to travel through the optical system with constant pulse duration, temporal focusing broadens the pulse duration along with the propagation path, and the pulse reaches the shortest duration only at the focal plane of the objective. This approach, also called plane-projection multiphoton microscopy, enables video-rate wide-field optical sectioning of live tissues^[69]. Rapid 3D imaging of living cells has been achieved using novel Bessel beam plane illumination microscopy^[70]. A Bessel beam has a relatively long focusing waist compared to a conventional Gaussian beam. Coupled with structural illumination and two-photon excitation, this method provides isotropic resolution of 0.3 μm and rapid imaging speed of 200 frames per second, thereby enabling 3D imaging of subcellular features.

3.3 Microendoscope

To further extend TPM for *in vivo* and internal tissue imaging, several two-photon microendoscopes using a gradient-index (GRIN) rod lens, miniature compound lens, or a fiber bundle have been developed^[71–80]. In these designs, the GRIN rod lens or fiber bundles relay the light from the proximal end of the endoscope to the distal end (in the tissue). Jung *et al.* developed a fast scanning endoscopy system based on a GRIN lens (0.46 NA, 1.8-mm diameter) and a microelectromechanical system (MEMS) scanner with mirror size of 750 \times 750 (μm)^[72,76,78]. Alternatively, Wu *et al.* developed a 2-mm-in-diameter all-fiber-optic endomicroscope

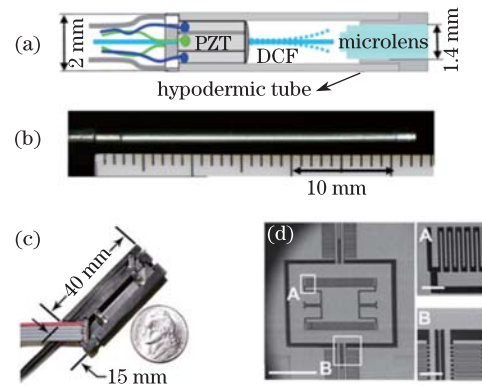


Fig. 3. Microendoscopes for TPM based on PZT and MEMS scanning systems. (a) Schematic and (b) photograph of the fiber-optic scanning two-photon endomicroscope probe including the PZT scanner, a single double-clad fiber (DCF), and miniature compound lens encased in a hypodermic tube with an overall dimension of 2 \times 32 (mm)^[80]. (c) Photograph shows the miniature probe using a MEMS mirror and a GRIN lens^[78]. (d) SEM micrographs of the MEMS scanning mirror design^[78]. The scale bars are 600 μm in (d) and 120 μm in inset.

using a piezoelectric transducer (PZT) scanner at the distal tip^[79,80]. Rivera *et al.* developed a compact and flexible raster scanning multiphoton endoscope capable of imaging unstained tissue^[77]. Figure 3 illustrates two-photon micro-endoscopes based on PZT and MEMS scanning systems.

4. Biomedical applications

4.1 Molecular imaging

For biomedical studies, TPM can probe molecular information such as calcium, ROS, glutamate, NADH, FAD, oxygen, among others^[28,42–45,81–86]. It was recently demonstrated that TPM could also excite fluorescence directly from hemoglobin^[87,88], allowing investigators to directly visualize microvasculature. The rich biological information provided by TPM makes it an attractive tool for various biomedical imaging applications.

Calcium is an indicator for neuron activity and also involved in the regulation of a variety of biological functions in cancer cells, including growth inhibition, drug resistance, etc.^[84,89]. TPM is a powerful means for monitoring the activity of distinct neurons in brain tissue with exquisite spatial and temporal resolution^[81,84,85].

Cellular metabolism involves a series of various biological processes, including energy metabolism, antioxidant/generation of oxidative stress, gene expression, cell death, immunological functions, aging, and carcinogenesis. The intracellular coenzyme NADH has been used as an intrinsically fluorescent indicator for cellular metabolic states, metabolic transitions, cancer detection, tissue oxygen supply, and hypoxia in hippocampal tissue slices^[14,18,45,82,83]. TPM of NADH provides high sensitivity and spatial resolution in three dimensions to resolve metabolic signatures in processes of astrocytes and neurons deep in highly scattering brain tissue slices^[82,83]. Recent work reported that NADH was also a photobiological metric of cell death and therapeutic effect^[42–44].

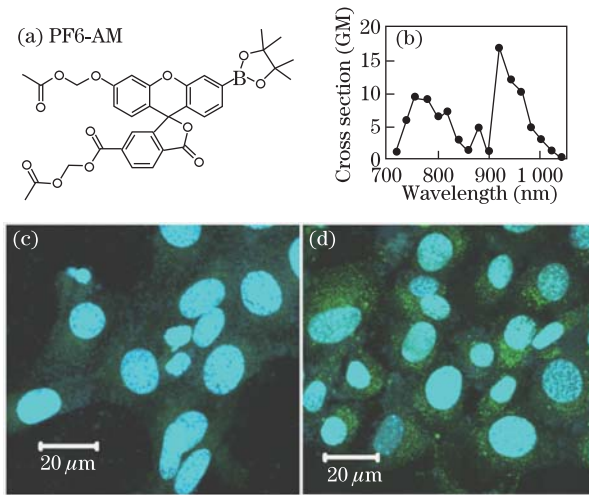


Fig. 4. (Color online) TPM imaging of H_2O_2 with chemoselective fluorescent probe PF6-AM^[8]. (a) Small-molecule probe PF6-AM; (b) two-photon cross sections for PF6-AM in H_2O_2 solution; TPM of endogenous H_2O_2 (green) in HT22 cells at (c) 6 and (d) 60 min after the addition of rotenone. The cells are loaded with 5 $\mu\text{mol/L}$ PF6-AM for 30 min before use.

ROS are generated as by-products of cellular metabolism, primarily in the mitochondria. It is an oxidative stress indicator related to cancer, diabetes, and neurodegenerative diseases. Recent evidence has shown that H_2O_2 , one of ROS, plays a key role as an intracellular second messenger in a variety of signaling transduction processes^[8,90,91]. To monitor the production of intracellular H_2O_2 , Guo *et al.* developed a protocol based on TPM and designed the fluorescent probe peroxyfluor-6 acetoxymethyl ester (PF6-AM), a new chemoselective indicator for H_2O_2 over other ROS^[8,90]. Figures 4(a) and (b) illustrate the fluorescence probe PF6-AM and its two-photon absorption spectrum. For the generation of intracellular H_2O_2 production, HT22 cells were incubated with PF6-AM and treated with rotenone, which is a mitochondrial complex I inhibitor that induces mitochondrial H_2O_2 production. Figures 4(c) and (d) show the TPM images of endogenous H_2O_2 (green) in HT22 cells. The nuclei (blue), stained with Hoechst 33342, were co-excited with 770-nm wavelength laser pulses^[8].

4.2 Applications in neuroscience

TPM has been used for high-resolution *in vivo* imaging of cellular morphology and activity, particularly of population activity in complex neuronal circuits and blood vessels. Representative active research topics include the stimulation of neuron circuit^[7,9,92] and physiological research of neurodegenerative diseases such as stroke and Alzheimer's disease^[13,93].

Stroke is the leading cause of death and disability around the world^[94]. TPM was reported for real-time monitoring of individual blood vessels surrounding cortical ischemia^[93]. Here, we demonstrate the application of TPM for imaging the recovery of mouse stroke model. Cortical vasculature, neurons, as well as their dendrites and spines in the peri-infarct cortex can be visualized in ischemic mice brains. This is important to understand the process of functional recovery, since

peri-infarct area is critical for rehabilitation. Figure 5 shows the TPF imaging of a mouse brain synaptogenesis for the evaluation of the injury area in a preclinical mouse stroke model. C57 BL/6J mice were subjected to the proximal middle cerebral artery occlusion (MCAO) for 30 min^[95,96]. Two months after MCAO, brains tissue sections were collected of 100- μm thickness using a vibrotome (Leica). Synaptophysin, labeled with Alexa Fluor 594, is a marker for synaptogenesis^[97]. This experiment demonstrated the synaptogenesis occurred at the peri-injury recovery area where synaptophysin expression significantly increased.

TPM enables deep tissue cortical vasculature imaging in a mouse brain *in vivo*. Using long wavelength 1 280-nm laser excitation, Kobat *et al.* achieved an imaging depth up to 1.6 mm in a mouse cortex, approximately reaching the fundamental depth limit in scattering tissue^[3]. Chia *et al.* developed a technique to produce high-quality images deep into the mouse neocortex by inserting a 1-mm right-angle glass microp prism into the neocortex^[98]. *In vivo* TPM imaging provides neuroscientists a new tool for investigating brain function and neural connectivity, and will ultimately improve treatment of developmental disorders, aging, and other diseases of the brain.

4.3 Applications in cancer diagnosis

Application of TPM to translational and clinical cancer research has burgeoned over the last several years. Most cancers begin as precancerous lesions that are

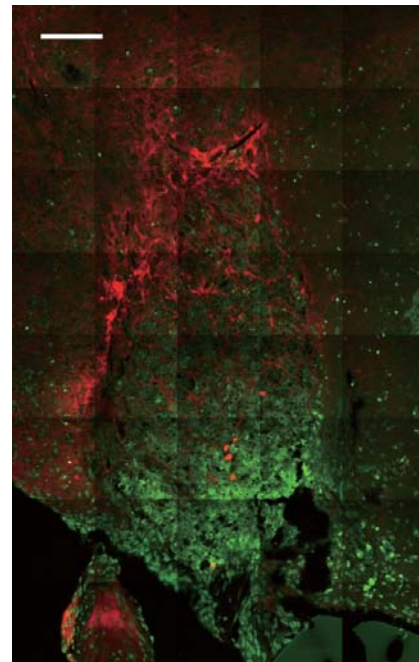


Fig. 5. (Color online) TPF imaging of mouse brain synaptogenesis is evaluated at adjacent the injury area at 2 months after ischemia *in vivo*. The expression of synaptophysin, labeled with Alexa Fluor 594 (pseudo red color), is used as a marker to evaluate synaptogenesis. The fluorophore is excited with a 770-nm, 80-MHz, and 140-fs Ti:sapphire laser (Coherent Chameleon Vision II). Autofluorescence (pseudo green color) is also detected with two-photon excitation. Scale bar: 100 μm .

located in the surface epithelium, which can be detected using TPM. For early cancer diagnosis, recent studies have demonstrated that morphological and fluorescence quantification from TPM can be used to distinguish cancerous and precancerous tissue from normal tissue^[18]. In this review, we focus on two forms of TPM, TPF and SHG imagings, as they have been used for investigating cancer pathology in both *ex vivo* and *in vivo* settings.

Without fluorescent staining, Zhuo *et al.* has been using two-photon autofluorescence and SHG microscopy to monitor colonic cancer progression, differentiate between normal and dysplastic human colonic tissues and probe the changes of basement membranes in different colonic cancer stages^[45,99,100]. They visualized cellular and sub-cellular details in colonic cancer progression, quantitatively monitored colonic cancer progression by both qualitative, label-free multiphoton imaging and quantitative redox analysis, and demonstrated the capability of label-free monitoring colonic cancer progression using TPM as an *in situ* histological tool. In addition, for the purpose of discriminating between normal and dysplastic colonic mucosa, they also demonstrated the potential of intrinsic SHG imaging to provide biochemical and morphological biomarkers, including the collagen density and the collagen fiber direction. Furthermore, *en face* SHG images from normal, precancerous and cancerous colonic tissues were acquired from 72 colonic biopsy specimens in order to probe the changes of basement membranes in different colonic cancer stages. In their results (Fig. 6), a honeycomb arrangement of round-shaped regular basement membranes with uniform size is observed in the normal case and the tubular-shaped basement membranes with larger size and a lower population density are obtained in precancerous tissues, but the basement membranes are vanished in cancer. In addition, among the normal, precancerous and cancerous tissues categories based on the unpaired Wilcoxon ranks sum test, significant differences were found in the circle length and population density of basement membranes variables^[45].

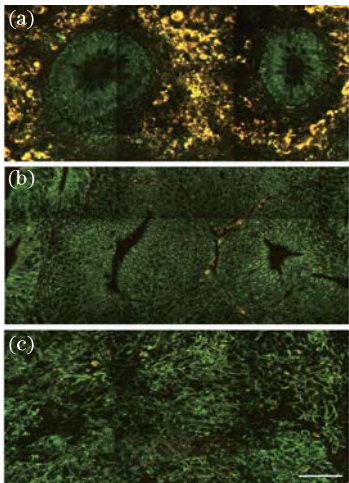


Fig. 6. (Color online) Representative TPF images from the (a) normal, (b) precancerous, and (c) cancerous colonic tissues^[45]. The excitation wavelength is 800 nm. NADH and FAD fluorescence signals are detected from green (430–490 nm) and red (500–560 nm) color-coded channels, respectively. Scale bar=50 μm .

5. Discussion

TPM has become one of the most powerful imaging methods for biomedical applications. Furthermore, the two-photon nonlinear process is a key technique to improve many optical technologies. Two-photon fluorescence resonance energy transfer (TP-FRET) can be used to image protein-protein interactions in cells^[101]. Combined with fluorescence correlation spectroscopy (FCS)^[102,103], TP-FCS provides automatic selection of a subvolume in a bulk sample, clear separation between excitation and emission wavelengths, and reduced photobleaching. With the help of suitable fluorescent probes, two-photon fluorescence lifetime imaging microscopy (TP-FLIM) with time-correlated single-photon counting can quantify the binding fraction in single dendritic spines^[104]. TP-FLIM has been demonstrated to play a prominent role in dissecting neuronal signaling mechanisms *in vivo*. To track molecular movements it is necessary to tag the molecules of interest in specific locations. In addition, fluorescence lifetime measurements can be easily combined with TPM to provide quantitative FRET imaging^[105]. TP-FRET-FLIM has also been demonstrated in biological applications^[106]. Another well-established method is to measure the fluorescence recovery after the photobleaching (FRAP). Using two-photon photobleaching, diffusion of biochemical substances through the spine neck has been measured^[85,107].

Sub-diffraction resolution in TPM was achieved by merging this technique with stimulated-emission depletion (STED)^[108,109]. Images of fluorescent nanoparticles and the immunostained transcription regulator NF κ B in mammalian cell nuclei exhibit resolutions of <50 nm and \sim 70 nm in the focal plane, respectively, corresponding to a 4–5.4-fold improvement over the diffraction barrier^[108]. Adaptive optics is promising to help compensate for scattering to further improve optical resolution and imaging depth^[110,111].

The combination of light microscopy and optogenetics actuators and reporters offers the possibility to control activation and inhibition of neuronal activity and monitor functional responses in a non-invasive manner enabling the analysis of well-defined neuronal populations within intact neuronal circuits and systems^[112–114]. Interestingly, these tools have permitted research to address key biological questions with relatively simple illumination methods using widefield visible light illumination. However, some limitations in the specificity of genetic targeting and the intricate morphology of the brain (neuronal processes, such as dendrites and axons, can reach regions far away from the cell soma) make it challenging to, for example, individuate subsets of genetically identical interconnected cells, or establish the role of specific spatiotemporal excitatory patterns in guiding animal behavior. To reach such degree of specificity, more sophisticated illumination methods are required, permitting control of light patterning deep inside tissues. TPM was recently presented for high-resolution patterned photoactivation of optogenetics molecules based on the temporal control of ultrafast pulses for axial localization of the illumination pattern^[112–114]. Two-photon illumination activates Channelrhodopsin-2 in mouse cul-

tured neurons and cortical slices with sufficient efficacy to reliably fire action potentials with millisecond temporal resolution and low excitation power when the light was shaped over the cell body, one or more dendritic subdomains or multiple cells simultaneously.

6. Conclusion

TPM is an emerging technology that is contributing to discoveries in biological studies on many spatiotemporal scales. Benefits from the developments in optical physics and optoelectronics, lead to technical advances that continue to overcome the limits of TPM. Combining TPM with other imaging techniques, such as optical coherence tomography (OCT)^[115–119] and Raman microscopy^[120,121] will allow the development of multimodal microscopes for imaging on live animals for behavioral research. The development of biocompatible synthetic fluorophores and transgene mouse models for specific molecular imaging would have a profound impact on biomedical research. The continuous evolving two-photon methodologies will help translate cancer research from the bench to the bedside, and ultimately bring minimally invasive methods for cancer diagnosis and treatment to therapeutic reality.

We thank Hsing-Wen Wang, Chia-Pin Liang, Nicholas Woolsey, and Renee E. Haskew-Layton for helpful discussions and comments; Chao-Wei Chen and Jianting Wang for technical assistance and cells culture; Chris Chang for the development of H₂O₂ probes. H. Guo and Y. Chen are supported by National Institutes of Health (NIH) under Grant Nos. R21AG042700, R21DK088066, and R21EB012215. L. Qin and S. Cho are supported by NIH under Grant No. R01HL082511. H. Aleyasin and R. R. Ratan are supported by NIH under Grant Nos. P01 AG 14930-10, NS04059, and NS39170. W. Gong, J. Chen, and S. Xie are supported by the National Natural Science Foundation of China under Grant No. 60678054.

References

- W. Denk, J. H. Strickler, and W. W. Webb, *Science* **248**, 73 (1990).
- D. Kobat, M. E. Durst, N. Nishimura, A. W. Wong, C. B. Schaffer, and C. Xu, *Opt. Express* **17**, 13354 (2009).
- D. Kobat, N. G. Horton, and C. Xu, *J. Biomed. Opt.* **16**, 106014 (2011).
- Y. Chen, C. P. Liang, Y. Liu, A. H. Fischer, A. V. Parwani, and L. Pantanowitz, *J. Pathol. Inform.* **3**, 22 (2012).
- W. R. Zipfel, R. M. Williams, and W. W. Webb, *Nat. Biotechnol.* **21**, 1369 (2003).
- K. Svoboda and R. Yasuda, *Neuron* **50**, 823 (2006).
- A. C. Kwan and Y. Dan, *Current Biology* **22**, 1459 (2012).
- H. Guo, H. Aleyasin, S. Howard, B. C. Dickinson, R. Haskew-Layton, D. Kobat, V. S. Lin, D. Rivera, C. J. Chang, R. R. Ratan, and C. Xu, in *Proceedings of Optical Molecular Probes, Imaging and Drug Delivery 2011* OtuD3 (2011).
- Y. Li, H. Lu, P. L. Cheng, S. Ge, H. Xu, S. H. Shi, and Y. Dan, *Nature* **486**, 118 (2012).
- D. Huber, D. A. Gutnisky, S. Peron, D. H. O'Connor, J. S. Wiegert, L. Tian, T. G. Oertner, L. L. Looger, and K. Svoboda, *Nature* **484**, 473 (2012).
- T. Ladewig, P. Kloppenburg, P. M. Lalley, W. R. Zipfel, W. W. Webb, and B. U. Keller, *J. Physiol.* **547**, 775 (2003).
- M. E. McLellan, S. T. Kajdasz, B. T. Hyman, and B. J. Bacskai, *J. Neurosci.* **23**, 2212 (2003).
- M. Meyer-Luehmann, T. L. Spire-Jones, C. Prada, M. Garcia-Alloza, A. de Calignon, A. Rozkalne, J. Koenigsknecht-Talboo, D. M. Holtzman, B. J. Bacskai, and B. T. Hyman, *Nature* **451**, 720 (2008).
- M. C. Skala, K. M. Ricking, A. Gendron-Fitzpatrick, J. Eickhoff, K. W. Eliceiri, J. G. White, and N. Ramanujam, *Proc. Natl. Acad. Sci. USA* **104**, 19494 (2007).
- H.-C. Guo, K. Takashima, A. Sato, H. Yokoyama, M. Mure, Y. Iseki, and H. Tsubokawa, *Proc. SPIE* **6860**, 686020 (2008).
- D. M. McDonald and P. L. Choyke, *Nat. Med.* **9**, 713 (2003).
- W. Wang, J. B. Wyckoff, V. C. Frohlich, Y. Oleynikov, S. Huttelmaier, J. Zavadil, L. Cermak, E. P. Bottinger, R. H. Singer, J. G. White, J. E. Segall, and J. S. Condeelis, *Cancer Res.* **62**, 6278 (2002).
- M. C. Skala, J. M. Squirrell, K. M. Vrotsos, V. C. Eickhoff, A. Gendron-Fitzpatrick, K. W. Eliceiri, and N. Ramanujam, *Cancer Res.* **65**, 1180 (2005).
- R. K. Jain, L. L. Munn, and D. Fukumura, *Nat. Rev. Cancer* **2**, 266 (2002).
- S. W. Perry, R. M. Burke, and E. B. Brown, *Ann. Biomed. Eng.* **40**, 277 (2012).
- J. M. Squirrell, D. L. Wokosin, J. G. White, and B. D. Bavister, *Nat. Biotechnol.* **17**, 763 (1999).
- T. H. Harris, E. J. Banigan, D. A. Christian, C. Konradt, E. D. Tait Wojno, K. Norose, E. H. Wilson, B. John, W. Weninger, A. D. Luster, A. J. Liu, and C. A. Hunter, *Nature* **486**, 545 (2012).
- H. D. Moreau, F. Lemaitre, E. Terriac, G. Azar, M. Piel, A.-M. Lennon-Dumenil, and P. Bousso, *Immunity* **37**, 351 (2012).
- P. Steven, F. Bock, G. Huttmann, and C. Cursiefen, *PLoS One* **6**, e26253 (2011).
- G. D. Victoria, T. A. Schwickert, D. R. Fooksman, A. O. Kamphorst, M. Meyer-Hermann, M. L. Dustin, and M. C. Nussenzweig, *Cell* **143**, 592 (2010).
- M. D. Duncan, J. Reintjes, and T. J. Manuccia, *Opt. Lett.* **7**, 350 (1982).
- H. Yokoyama, A. Sato, H. C. Guo, K. Sato, M. Murc, and H. Tsubokawa, *Opt. Express* **16**, 17752 (2008).
- S. Sakadzic, E. Roussakis, M. A. Yaseen, E. T. Mandeville, V. J. Srinivasan, K. Arai, S. Ruvinskaya, A. Devor, E. H. Lo, S. A. Vinogradov, and D. A. Boas, *Nat. Methods* **7**, 755 (2010).
- X. K. Shu, A. Royant, M. Z. Lin, T. A. Aguilera, V. Lev-Ram, P. A. Steinbach, and R. Y. Tsien, *Science* **324**, 804 (2009).
- N. C. Shaner, P. A. Steinbach, and R. Y. Tsien, *Nat. Methods* **2**, 905 (2005).
- D. Shcherbo, I. I. Shemiakina, A. V. Ryabova, K. E. Luker, B. T. Schmidt, E. A. Souslova, T. V. Gorodnicheva, L. Strukova, K. M. Shidlovskiy, O. V. Britanova, A. G. Zarausky, K. A. Lukyanov, V. B. Loschenov, G. D. Luker, and D. M. Chudakov, *Nat. Methods* **7**, 827 (2010).
- P. S Weiss, *ACS Nano* **2**, 1977 (2008).
- A. Roda, *Anal. Bioanal. Chem.* **396**, 1619 (2010).
- D. R. Larson, W. R. Zipfel, R. M. Williams, S. W. Clark,

- M. P. Bruchez, F. W. Wise, and W. W. Webb, *Science* **300**, 1434 (2003).
35. J. Park, A. Estrada, K. Sharp, K. Sang, J. A. Schwartz, D. K. Smith, C. Coleman, J. D. Payne, B. A. Korgel, A. K. Dunn, and J. W. Tunnell, *Opt. Express* **16**, 1590 (2008).
 36. L. Cao, X. Wang, M. J. Meziani, F. S. Lu, H. F. Wang, P. J. G. Luo, Y. Lin, B. A. Harruff, L. M. Veca, D. Murray, S. Y. Xie, and Y. P. Sun, *J. Am. Chem. Soc.* **129**, 11318 (2007).
 37. A. H. Fu, W. W. Gu, C. Larabell, and A. P. Alivisatos, *Curr. Opin. Neurobiol.* **15**, 568 (2005).
 38. R. E. Rumbaut and A. J. Sial, *Microcirculation* **6**, 205 (1999).
 39. A. M. Derfus, W. C. W. Chan, and S. N. Bhatia, *Nano Lett.* **4**, 11 (2004).
 40. M. P. Jain, A. O. Choi, K. D. Nebibert, and D. Maysinger, *Nanomed.* **4**, 277 (2009).
 41. W. R. Zipfel, R. M. Williams, R. Christie, A. Y. Nikitin, B. T. Hyman, and W. W. Webb, *Proc. Natl. Acad. Sci USA* **100**, 7075 (2003).
 42. G. C. Su, Y. H. Wei, and H. W. Wang, *Opt. Express* **19**, 21145 (2011).
 43. H. W. Guo, C. T. Chen, Y. H. Wei, O. K. Lee, V. Gukassyan, F. J. Kao, and H. W. Wang, *J. Biomed. Opt.* **13**, 050505 (2008).
 44. H. W. Guo, Y. H. Wei, and H. W. Wang, *J. Biomed. Opt.* **16**, 068001 (2011).
 45. S. M. Zhuo, J. Yan, G. Chen, J. X. Chen, Y. C. Liu, J. P. Lu, X. Q. Zhu, X. S. Jiang, and S. S. Xie, *Biomed. Opt. Express* **2**, 615 (2011).
 46. P. J. Campagnola and L. M. Loew, *Nat. Biotechnol.* **21**, 1356 (2003).
 47. A. Zumbusch, G. R. Holtom, and X. S. Xie, *Phys. Rev. Lett.* **82**, 4142 (1999).
 48. J.-X. Cheng and X. S. Xie, *J. Phys. Chem. B* **108**, 827 (2004).
 49. C. Xu and W. W. Webb, *J. Opt. Soc. Am. B* **13**, 481 (1996).
 50. M. Balu, T. Baldacchini, J. Carter, T. B. Krasieva, R. Zadoyan, and B. J. Tromberg, *J. Biomed. Opt.* **14**, 010508 (2009).
 51. H. Guo, K.-I. Sato, K. Takashima, and H. Yokoyama, in *Proceedings of International Conference on Ultrafast Phenomena 2006* TuE8 (2006).
 52. H. Yokoyama, H. Guo, T. Yoda, K. Takashima, K. Sato, H. Taniguchi, and H. Ito, *Opt. Express* **14**, 3467 (2006).
 53. M. Kuramoto, N. Kitajima, H. Guo, Y. Furushima, M. Ikeda, and H. Yokoyama, *Opt. Lett.* **32**, 2726 (2007).
 54. S. W. Chu, I. H. Chen, T. M. Liu, P. C. Chen, C. K. Sun, and B. L. Lin, *Opt. Lett.* **26**, 1909 (2001).
 55. C. Wang, L. Qiao, F. He, Y. Cheng, and Z. Xu, *J. Microsc-Oxford* **243**, 179 (2011).
 56. C. Wang, L. L. Qiao, Z. L. Mao, Y. Cheng, and Z. Z. Xu, *J. Opt. Soc. Am. B* **25**, 976 (2008).
 57. K. Murari, Y. Y. Zhang, S. P. Li, Y. P. Chen, M. J. Li, and X. D. Li, *Opt. Lett.* **36**, 1299 (2011).
 58. S. Yazdanfar, C. Joo, C. Zhan, M. Y. Berezin, W. J. Akers, and S. Achilefu, *J. Biomed. Opt.* **15**, 030505 (2010).
 59. H. Yokoyama, H. Tsubokawa, H. Guo, J. Shikata, K. Sato, K. Takashima, K. Kashiwagi, N. Saito, H. Taniguchi, and H. Ito, *J. Biomed. Opt.* **12**, 054019 (2007).
 60. K. Taira, T. Hashimoto, and H. Yokoyama, *Opt. Express* **15**, 2454 (2007).
 61. J. R. Unruh, E. S. Price, R. G. Molla, L. Stehno-Bittel, C. K. Johnson, and R. Hui, *Opt. Express* **14**, 9825 (2006).
 62. R. Aviles-Espinosa, Y. Ding, M. A. Cataluna, D. Nikitichev, P. Loza-Alvarez, and E. Rafailov, in *Proceedings of CLEO: Applications and Technology* ATH1M.2 (2012).
 63. G. D. Reddy and P. Saggau, *J. Biomed. Opt.* **10**, 064038 (2005).
 64. R. H. Jiang, X. H. Lu, D. R. Li, T. W. Quan, X. L. Liu, Q. M. Luo, and S. Q. Zeng, *Prog. Biochem. Biophys.* **39**, 505 (2012).
 65. K. H. Kim, C. Buehler, K. Bahlmann, T. Ragan, W. C. Lee, E. Nedivi, E. L. Heffer, S. Fantini, and P. T. So, *Opt. Express* **15**, 11658 (2007).
 66. S. S. Howard, A. A. Straub, and C. Xu, in *Proceedings of CLEO CWD6* (2010).
 67. A. A. Straub, S. S. Howard, and C. Xu, in *Proceedings of CLEO: Applications and Technology* ATh4C.3 (2012).
 68. D. Oron, E. Tal, and Y. Silberberg, *Opt. Express* **13**, 1468 (2005).
 69. J. Y. Yu, C. H. Kuo, D. B. Holland, Y. Chen, M. Ouyang, G. A. Blake, R. Zadoyan, and C. L. Guo, *J. Biomed. Opt.* **16**, 116009 (2011).
 70. T. A. Planchon, L. Gao, D. E. Milkie, M. W. Davidson, J. A. Galbraith, C. G. Galbraith, and E. Betzig, *Nature Methods* **8**, 417 (2011).
 71. P. Kim, M. Puoris'haag, D. Cote, C. P. Lin, and S. H. Yun, *J. Biomed. Opt.* **13**, 010501 (2008).
 72. J. C. Jung and M. J. Schnitzer, *Opt. Lett.* **28**, 902 (2003).
 73. G. J. Liu, T. Q. Xie, I. V. Tomov, J. P. Su, L. F. Yu, J. Zhang, B. J. Tromberg, and Z. P. Chen, *Opt. Lett.* **34**, 2249 (2009).
 74. W. Gobel, J. N. Kerr, A. Nimmerjahn, and F. Helmchen, *Opt. Lett.* **29**, 2521 (2004).
 75. M. J. Levene, D. A. Dombeck, K. A. Kasischke, R. P. Molloy, and W. W. Webb, *J. Neurophys.* **91**, 1908 (2004).
 76. W. Piyawattanametha, R. P. Barretto, T. H. Ko, B. A. Flusberg, E. D. Cocker, H. Ra, D. Lee, O. Solgaard, and M. J. Schnitzer, *Opt. Lett.* **31**, 2018 (2006).
 77. D. R. Rivera, C. M. Brown, D. G. Ouzounov, I. Pavlova, D. Kobat, W. W. Webb, and C. Xu, *Proc. Natl. Acad. Sci. USA* **108**, 17598 (2011).
 78. C. L. Hoy, N. J. Durr, P. Y. Chen, W. Piyawattanametha, H. Ra, O. Solgaard, and A. Ben-Yakar, *Opt. Express* **16**, 9996 (2008).
 79. Y. Wu, Y. Leng, J. Xi, and X. Li, *Opt. Express* **17**, 7907 (2009).
 80. Y. Y. Zhang, M. L. Akins, K. Murari, J. F. Xi, M. J. Li, K. Luby-Phelps, M. Mahendroo, and X. D. Li, *Proc. Natl. Acad. Sci. USA* **109**, 12878 (2012).
 81. W. Denk, *Proc. Natl. Acad. Sci. USA* **91**, 6629 (1994).
 82. K. A. Kasischke, H. D. Vishwasrao, P. J. Fisher, W. R. Zipfel, and W. W. Webb, *Science* **305**, 99 (2004).
 83. H. D. Vishwasrao, A. A. Heikal, K. A. Kasischke, and W. W. Webb, *J. Biol. Chem.* **280**, 25119 (2005).
 84. C. Stosiek, O. Garaschuk, K. Holthoff, and A. Konnerth, *Proc. Natl. Acad. Sci. USA* **100**, 7319 (2003).
 85. A. Sobczyk, V. Scheuss, and K. Svoboda, *J. Neurosci.* **25**, 6037 (2005).
 86. A. Cheng, J. T. Goncalves, P. Golshani, K. Arisaka, and C. Portera-Cailliau, *Nat. Methods* **8**, 139 (2011).
 87. W. Zheng, D. Li, Y. Zeng, Y. Luo, and J. Y. Qu, *Biomed.*

- Opt. Express **2**, 71 (2010).
88. D. Li, W. Zheng, Y. Zeng, Y. Luo, and J. Y. Qu, Opt. Lett. **36**, 834 (2011).
89. M. A. DeBernardi and G. Brooker, Method Enzymol. **414**, 317 (2006).
90. B. C. Dickinson, J. Peltier, D. Stone, D. V. Schaffer, and C. J. Chang, Nat. Chem. Biol. **7**, 106 (2011).
91. J. R. Stone and S. Yang, Antioxid Redox Signal **8**, 243 (2006).
92. M. A. Go, C. Stricker, S. Redman, H.-A. Bachor, and V. R. Daria, J. Biophoton. **5**, 745 (2012).
93. N. Nishimura, C. B. Schaffer, B. Friedman, P. S. Tsai, P. D. Lyden, and D. Kleinfeld, Nat. Methods **3**, 99 (2006).
94. J. Bosch, S. Yusuf, J. Pogue, P. Sleight, E. Lonn, B. Rangoonwala, R. Davies, J. Ostergren, J. Probstfield, and H. Investigators, Brit. Med. J. **324**, 699 (2002).
95. S. Cho, E. M. Park, M. Febbraio, J. Anrather, L. Park, G. Racchumi, R. L. Silverstein, and C. Iadecola, J. Neurosci. **25**, 2504 (2005).
96. Y. Bao, L. Y. Qin, E. Kim, S. Bhosle, H. C. Guo, M. Febbraio, R. E. Haskew-Layton, R. Ratan, and S. Cho, J. Cerebr. Blood Flow Met. **32**, 1567 (2012).
97. H. Ujike, M. Takaki, M. Kodama, and S. Kuroda, Ann. Ny. Acad. Sci. **965**, 55 (2002).
98. T. H. Chia and M. J. Levene, J. Neurophys. **102**, 1310 (2009).
99. S. Zhuo, X. Zhu, G. Wu, J. Chen, and S. Xie, J. Biomed. Opt. **16**, 120501 (2011).
100. S. Zhuo, J. Yan, G. Chen, H. Shi, X. Zhu, J. Lu, J. Chen, and S. Xie, Plos One **7**, e38655 (2012).
101. M. Elangovan, H. Wallrabe, Y. Chen, R. N. Day, M. Barroso, and A. Periasamy, Methods **29**, 58 (2003).
102. K. M. Berland, P. T. C. So, and E. Gratton, Biophys. J. **68**, 694 (1995).
103. S. A. Kim, K. G. Heinze, and P. Schwille, Nat Methods **4**, 963 (2007).
104. R. Yasuda, C. D. Harvey, H. Zhong, A. Sobczyk, L. van Aelst, and K. Svoboda, Nat. Neurosci. **9**, 283 (2006).
105. Y. E. Chen and A. Periasamy, Microsc. Res. Techniq. **63**, 72 (2004).
106. A. Jeshtadi, P. Burgos, C. D. Stubbs, A. W. Parker, L. A. King, M. A. Skinner, and S. W. Botchway, J. Virol **84**, 12886 (2010).
107. K. Kucharz, T. Wieloch, and H. Toresson, J. Cereb Blood Flow Met. **31**, 1663 (2011).
108. G. Moneron and S. W. Hell, Opt. Express **17**, 14567 (2009).
109. P. Bianchini and A. Diaspro, J. Microsc-Oxford **245**, 225 (2012).
110. N. Jia, T. R. Sato, and E. Betzig, Proc. Natl. Acad. Sci. USA **109**, 22 (2012).
111. N. Ji, D. E. Milkie, and E. Betzig, Nat. Methods **7**, 141 (2010).
112. E. Papagiakoumou, F. Anselmi, A. Begue, V. de Sars, J. Gluckstad, E. Y. Isacoff, and V. Emiliani, Nat. Methods **7**, 848 (2010).
113. B. K. Andrasfalvy, B. V. Zemelman, J. Tang, and A. Vaziri, Proc. Natl. Acad. Sci. USA **107**, 11981 (2010).
114. J. P. Rickgauer and D. W. Tank, Proc. Natl. Acad. Sci. USA **106**, 15025 (2009).
115. S. A. Yuan, C. A. Roney, J. Wierwille, C. W. Chen, B. Y. Xu, G. Griffiths, J. Jiang, H. Z. Ma, A. Cable, R. M. Summers, and Y. Chen, Phys. Med. Biol. **55**, 191 (2010).
116. J. Xi, K. Murari, Y. Zhang, Y. Chen, J. Li, and X. Li, in *Proceedings of Bio-Optics: Design and Application BWA5* (2011).
117. B. Jeong, B. Lee, M. S. Jang, H. Nam, S. J. Yoon, T. Wang, J. Doh, B. G. Yang, M. H. Jang, and K. H. Kim, Opt. Express **19**, 13089 (2011).
118. C. Vinegoni, T. Ralston, W. Tan, W. Luo, D. L. Marks, and S. A. Boppart, Appl. Phys. Lett. **88**, 053901 (2006).
119. S. Tang, C. H. Sun, T. B. Krasieva, Z. P. Chen, and B. J. Tromberg, Opt. Lett. **32**, 503 (2007).
120. J. Kneipp, H. Kneipp, and K. Kneipp, Proc. Natl. Acad. Sci. USA **103**, 17149 (2006).
121. C. H. Chien, W. W. Chen, J. T. Wu, and T. C. Chang, J. Biomed. Opt. **16**, 016012 (2011).